Research on Chemical Intermediates (2023) 49:1463–1484
https://doi.org/10.1007/s11164-022-04908-1

New Schiff bases based on isatin and (thio)/carbohydrazone: preparation, experimental–theoretical spectroscopic characterization, and DFT approach to antioxidant characteristics

Halit Muğlu[1] · Fatih Sönmez[2] · M. Serdar Çavuş[3] · Belma Z. Kurt[4] · Hasan Yakan[5]

Received: 16 July 2022 / Accepted: 2 December 2022 / Published online: 21 December 2022

Abstract

In this study, synthesis, spectroscopic elucidation, and investigation of antioxidant properties of new Schiff bases based on isatin and (thio)/carbohydrazone derivatives have been reported for the first time. The structures of the synthesized compounds were elucidated by FT-IR, ^{1}H-NMR, and ^{13}C-NMR spectroscopic methods and elemental analysis. Their DPPH, ABTS, and CUPRAC activities were evaluated as antioxidant properties. Electronic and spectral data of the compounds were obtained by DFT calculations at the B3LYP/6–311++G(2d,2p) level of theory. Intramolecular interactions and charge densities on the bonds were analyzed by QTAIM and IRI calculations. In addition to parameters such as frontier molecular orbital energy eigenvalues, electronegativity, nucleophilicity index, and electrodonating power, the changes in the enthalpy of the compounds for the reactions realized through the SET mechanism were calculated to elucidate the antioxidant reactions of the compounds. Most of synthesized compounds exhibited antioxidant activities with the IC_{50} values ranging from 27.13 to 43.35 μM for DPPH, from 6.47 to 24.96 μM for ABTS and with the $A_{0.50}$ values ranging from 9.04 to 47.52 μM for CUPRAC. Among them, compound **3**, containing two hydroxyl groups, showed the strongest antioxidant activity for each assay (IC_{50} = 27.13 μM for DPPH, 6.47 μM for ABTS, and $A_{0.50}$ = 9.04 μM for CUPRAC). The antioxidant activities of compound **3** were almost two or threefold weaker than that of BHA (IC_{50} = 9.55 μM for DPPH, 3.42 μM for ABTS, and $A_{0.50}$ = 2.24 μM for CUPRAC), used as a standard. In addition, thiocarbohydrazone compounds exhibited higher antioxidant activity than carbohydrazones. Electron donating ability and single electron transfer enthalpy calculations predicted that thiocarbohydrazone compounds can perform SET reactions more easily than carbohydrazones.

Keywords Schiff bases · Isatin · Spectroscopic elucidation · Antioxidant assay · DFT

Extended author information available on the last page of the article

Introduction

Schiff base (CH=N–) compounds have a significant class of organic chemistry due to a wide range of medicinal, chemical, and biological activity. They have enzyme inhibitor [1], anticancer [2], antiinflammatory [3], magnetic properties [4], antioxidant [5–7], antimicrobial [8], antibacterial [9], and cytotoxic activity [10]. Schiff bases are also used in industry as corrosion inhibitors [11, 12].

Thio/carbohydrazones are another important group of synthetic organic chemistry. They have been reported pharmaceutical and biological properties such as antiviral [13], antitumor [14], antituberculosis [15], antileishmanial [16], antimicrobial [17], antibacterial [18], and antioxidant activity [19–22].

Preservation of the oxidant-antioxidant balance of the organism is necessary for maintaining a healthy life [23, 24]. Free radicals are produced endogenously during the normal metabolic process [25]. Moreover, exogenous factors such as radiation, sun rays, environmental pollution, and cigarettes also cause the formation of free radicals [26]. Due to their reactivity, free radicals have the potential to damage and interact with all cell components, especially lipids, nucleic acids, and proteins [27]. Oxidative stress can develop in the organism due to the increase in free radical formation and/or the deficiency in the antioxidant defense system [28]. Oxidative stress, which is one of the factors that cause many common diseases such as diabetes, cancer and aging, arises from the imbalance between reactive oxygen species (ROS) and the antioxidant defense system of the cell [29, 30]. While low levels of ROS show biological effects such as a defense mechanism against pathogenic microorganisms and intercellular communication, high concentrations of ROS cause damage to DNA, lipids and proteins, and even cell death [31, 32]. Therefore, the ROS level in the body should be kept at the right rate. To maintain this ratio, the antioxidant system is activated to reduce free radical toxicity [33]. However, exceeding the antioxidant defense system capacity and excessive presence of superoxide radical result in the formation of ROS [34]. In these cases, the use of natural or synthetic antioxidants may be necessary. Antioxidants have an important role in protecting people against many diseases by scavenging free radicals [35, 36]. Therefore, the design and synthesis of effective new antioxidants continue to be the focus of interest for scientists.

In this paper, new Schiff bases based on isatin and (thio)/carbohydrazone derivatives were obtained by reaction of isatin-(thio)carbohydrazides with various aromatic aldehydes. FT-IR, ^{1}H NMR, and ^{13}C NMR spectroscopic methods and elemental analysis were used to confirm the structures of all compounds. The DPPH, ABTS, and CUPRAC activities of the synthesized compounds were evaluated for antioxidant properties. Furthermore, DFT calculations were performed for the theoretical analysis of both spectral and antioxidant experimental data and to examine the consistency between them. The single electron transfer (SET) mechanism in the reactions of the compounds with DPPH is discussed, and some electronic parameters are calculated to analyze the relationship between SET and the electronic parameters of the compounds. The calculation data were used to determine the antioxidant properties of the compounds. Interaction reaction

indicator (IRI) maps were used to examine the intramolecular interactions of the compounds. The relationship of the charge densities of the bonds between the QTAIM data and IRI maps was also examined. Our group continues to work on the design, synthesis and various activities of carbohydrazone and isatin molecules. In this study, these molecules were designed to investigate the antioxidant effects of isatins containing different groups (H and Cl), sulfur or oxygenated carbohydrazones (S or O), and different aldehydes with phenolic structure, and their antioxidant effects were theoretically investigated using QTAIM and IRI analysis methods.

Materials and methods

Instruments and chemicals

All chemical materials were purchased from Sigma-Aldrich, Acros Organics, or Merck Chemical Company and were used without further purification. The solvents were of spectroscopic grade. A Stuart SMP 30 melting point apparatus was utilized for determining melting points °C. The elemental analysis was performed on a Eurovector EA3000-Single. A Bruker Alpha Fourier transform IR (FT-IR) spectrometer was used to record for infrared spectra. ^{1}H and ^{13}C NMR spectra were taken on a Bruker Avance DPX-400 spectrophotometer (400 and 101 MHz) in DMSO-d_6. Antioxidant spectrophotometric measurements were performed with BioTek Synergy H1 Hybrid Multi-Mode Reader.

Synthesis of new Schiff bases based on isatin and (thio)/carbohydrazone derivatives

A mixture of isatin (5.0 mmol) and thiocarbohydrazide or carbohydrazide (5.0 mmol) in ethanol (20 mL) and two drops hydrochloric acid was refluxed for 3 h. The mixture was cooled, and the precipitate formed was filtered and washed with ethanol (96%) to give isatin-β-(thio)carbohydrazides. A mixture of isatin-β-(thio) carbohydrazides (2.0 mmol), various aromatic aldehydes (2.0 mmol), and two drops hydrochloric acid in ethanol (20 mL) was refluxed for 3 h. The color precipitate formed was filtered and washed with ethanol (96%) to give a product. The reaction route is as given in Scheme 1. They were obtained with slight changes according to an earlier procedure [14].

Antioxidant activity assay

DPPH (1,1-diphenyl-2-picrylhydrazyl) radical scavenging activity, ABTS (2,2′-azino-bis(3-ethylbenzothiazoline-6-sulfonic acid diammonium salt)) scavenging activity and CUPRAC (cupric reducing antioxidant capacities) activity of the synthesized compounds were determined according to the literature methods [36–38]. The detailed

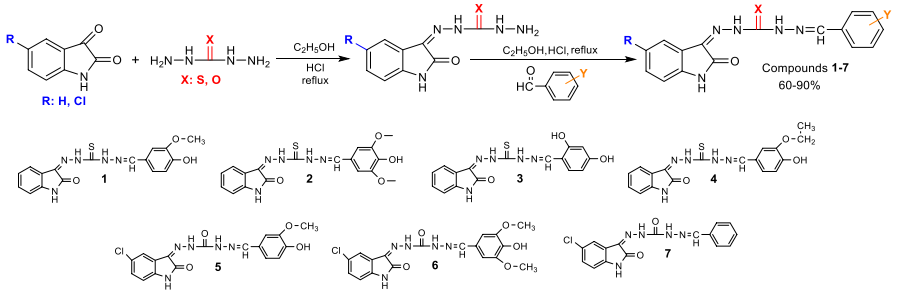

Scheme 1 Synthetic pathway for new Schiff bases derivatives (**1–7**)

procedures of antioxidant assays are given in Supporting Materials, under the experimental section.

Computational procedure

DFT [39, 40] calculations were performed at B3LYP/6–311++G(2d,2p) theory level using Gaussian09 software [41]. In the calculations, no symmetry restrictions on the compounds were used. Imaginary frequencies are not observed in the IR calculations, so the optimized state geometries correspond to the global minimum energy points on the potential energy surface. (Coordinates of optimized geometries of compounds are given in Supplementary Table S1.)

Since the experimental NMR data were taken in dimethyl sulfoxide (DMSO) environment, DFT/^{1}H-^{13}C NMR calculations were accordingly performed using the Gauge-independent atomic orbital (GIAO) method in the DMSO phase. Relative chemical shift values were obtained by subtracting the absolute chemical shielding of tetramethylsilane (TMS), calculated at the same level of theory (31.8149 and 183.737 ppm for ^{1}H and ^{13}C NMR, respectively).

The IR calculations were performed in the gas phase, and the electronic parameters of the compounds were also obtained from the gas phase calculations. Global chemical reactivity parameters such as HOMO-LOMO energy gap (ΔE), chemical hardness (η), electronegativity (χ), electrophilic index (ω), nucleophilic index (ε), and electrodonating power indices (ω^{-}) were obtained using frontier molecular orbital (FMO) energy eigenvalues. Furthermore, using Multiwfn software [42], QTAIM analysis [43, 44] to determine ring critical points (RCPs) of charge density distribution and bond critical points (BCPs) of bonded atoms, IRI calculations to visualize intramolecular interactions, and electron delocalization index (DI) calculations were performed.

Table 1 Physical data for the synthesized compounds

Comp	Compounds name's	-Y	M.P. (°C)	Color	Yield (%)
1	*N'*-(4-hydroxy-3-methoxybenzylidene)-2-((Z)-2-oxoindolin-3-ylidene)hydrazine-1-carbothiohydrazide	3-OCH_3-4-OH (X:S)	239–240	Yellow	90
2	*N'*-(4-hydroxy-3,5-dimethoxybenzylidene)-2-((Z)-2-oxoindolin-3-ylidene)hydrazine-1-carbothiohydrazide	3,5-diOCH_3-4-OH (X:S)	245–246	Light brown	79
3	*N'*-(2,4-dihydroxybenzylidene)-2-((Z)-2-oxoindolin-3-ylidene)hydrazine-1-carbothiohydrazide	2,4-diOH (X:S)	248–250	Yellow	88
4	*N'*-(3-ethoxy-4-hydroxybenzylidene)-2-((Z)-2-oxoindolin-3-ylidene)hydrazine-1-carbothiohydrazide	3-OC_2H_5-4-OH (X:S)	236–237	Yellow	80
5	*N'*-((Z)-5-chloro-2-oxoindolin-3-ylidene)-2-(4-hydroxy-3-methoxybenzylidene)hydrazine-1-carbohydrazide	3-OCH_3-4-OH (X:O)	249–250	Yellow	79
6	*N'*-((Z)-5-chloro-2-oxoindolin-3-ylidene)-2-(4-hydroxy-3,5-dimethoxybenzylidene)hydrazine-1-carbohydrazide	3,5-diOCH_3-4-OH (X:O)	272–274	Light brown	65
7	*N'*-benzylidene-2-((Z)-5-chloro-2-oxoindolin-3-ylidene)hydrazine-1-carbohydrazide	H (X:O)	278–280	Yellow	60

Table 2 Results for elemental analysis and solubility for the synthesized compounds

				Calculated			Experimental		
Comp	Solubility	Mol. weight g/mol	Mol. formula	C %	H %	N %	C %	H %	N %
1	DMSO (+)	369.0	$C_{17}H_{15}N_5O_3S$	55.28	4.09	18.96	55.40	4.03	19.05
2	DMSO (+)	399.0	$C_{18}H_{17}N_5O_4S$	54.13	4.29	17.53	54.26	4.22	17.66
3	DMSO (+)	355.0	$C_{16}H_{13}N_5O_3S$	54.08	3.69	19.71	53.92	3.75	19.82
4	DMSO (+)	383.0	$C_{18}H_{17}N_5O_3S$	56.39	4.47	18.27	56.25	4.52	18.33
5	DMSO (+)	387.5	$C_{17}H_{14}ClN_5O_4$	52.66	3.64	18.06	52.54	3.70	18.11
6	DMSO (+)	417.5	$C_{18}H_{16}ClN_5O_5$	51.75	3.86	16.76	51.87	3.90	16.60
7	DMSO (+)	341.5	$C_{16}H_{12}ClN_5O_2$	56.23	3.54	20.49	56.10	3.60	20.55

Results and discussion

Physical properties

Physical appearances, melting points, yields, and elemental analysis data of the compounds are summarized in Tables 1, 2.

Interpretation of vibrational frequencies

In the FTIR spectra of the synthesized compounds, both stretching peaks the aldehyde group (–CHO, two bands) and of the amino group ($–NH_2$) of the starting materials did not observed at 2780–2650 and 3570–3250 cm^{-1}, respectively. Instead, new peaks were observed at 1623–1585 cm^{-1}, resulting from the –C=N stretching vibrations of the azomethine (imine) group. At 1670–1607 cm^{-1}, theoretical values of these peaks were observed.

For all compounds **1**–**7**, amine group (–NH) vibration signals of isatin ring and thio/carbohydrazide moiety were detected at 3363–3197 and 3239–3128 cm^{-1}, respectively. Theoretical values of these amine peaks were observed at 3282–3281 and 3214–3093 cm^{-1}. For compounds **1**–**7**, –C=O signals of the isatin ring were observed at 1735–1685 cm^{-1} (theoretical values: 1711–1702 cm^{-1}), the –C–N stretching vibrations were detected at 1313–1205 cm^{-1} (theoretical values: 1671–1607 cm^{-1}). For compounds **1**–**6**, the –OH stretching vibrations were observed at 3521–3320 cm^{-1} (theoretical values: 3490–3310 cm^{-1}). For compounds **5**–**7**, –C=O signals of the carbohydrazide moiety were detected 1710–1688 cm^{-1} (theoretical value: 1787 cm^{-1}). For compounds **1**–**4**, the –C=S signals of the thiocarbohydrazide moiety were observed at 1388–1370 cm^{-1} (theoretical values: 1399–1390 cm^{-1}). For compounds **1**–**6**, the –C–O stretching vibrations were observed at 1186–1111 cm^{-1} (theoretical values: 1183–1050 cm^{-1}). For compounds **5**–**7**, –C–Cl signals were detected 1034–1001 cm^{-1} (all IR spectra are given in Figs. S1–S7). The experimental and theoretical IR peaks of the compounds are presented in Table 3. (Harmonic frequencies are calculated larger due to neglect of the

Table 3 Experimental and calculated IR vibration frequencies of the compounds

Comp. (tcrb/crb)	ν_{OH}	ν_{NH} (ist)	ν_{NH} (crb)	ν_{CH} (Ar)	$\nu_{C=O}$ (ist)	$\nu_{C=N}$	$\nu_{C=S/C=O}$	ν_{C-N}	ν_{C-O}	ν_{C-Cl}
Experimental										
1	3345	3287	3138	3056	1697	1620, 1601	1370	1236, 1220	1146, 1121	–
2	3484	3314	3155	3027	1695	1622, 1589	1388	1252, 1223	1159, 1111	–
3	3521	3202	3139	3071	1685	1622, 1601	1387	1255, 1239	1167, 1125	–
4	3320	3203	3176	3043	1701	1619, 1602	1372	1253, 1205	1163, 1122	–
5	3435	3363	3198	3097	1732	1619, 1589	1710	1309, 1282	1186, 1148	1028
6	3481	3284	3239	3080	1718	1623, 1592	1695	1313, 1283	1163, 1112	1001
7	–	3197	3128	3083	1735	1622, 1585	1688	1304, 1258	–	1034
Calculated										
1	3433	3281	3208, 3093	3089–3050	1702	1630, 1611	1399	1306, 1281	1183, 1049	–
2	3426	3281	3207, 3094	3095–3060	1702	1657, 1611	1390	1311, 1279	1118, 1055	–
3	3490, 3310	3281	3214, 3099	3078–3039	1708	1642, 1619	1396	1305, 1287	1174, 1154	–
4	3431	3282	3207, 3094	3090–3049	1702	1660, 1611	1398	1304, 1282	1145, 1053	–
5	3434	3282	3212, 3129	3091–3050	1704	1637, 1607	1787	1294, 1235	1183, 1050	1086
6	3427	3282	3211, 3129	3096–3061	1704	1627, 1607	1787	1291, 1264	1175, 1114	1085
7	–	3281	3208, 3121	3076–3037	1711	1671, 1613	1787	1292, 1265	–	1085

tcrb thiocarbohydrazone, *crb* carbohydrazone, *ist* isatin

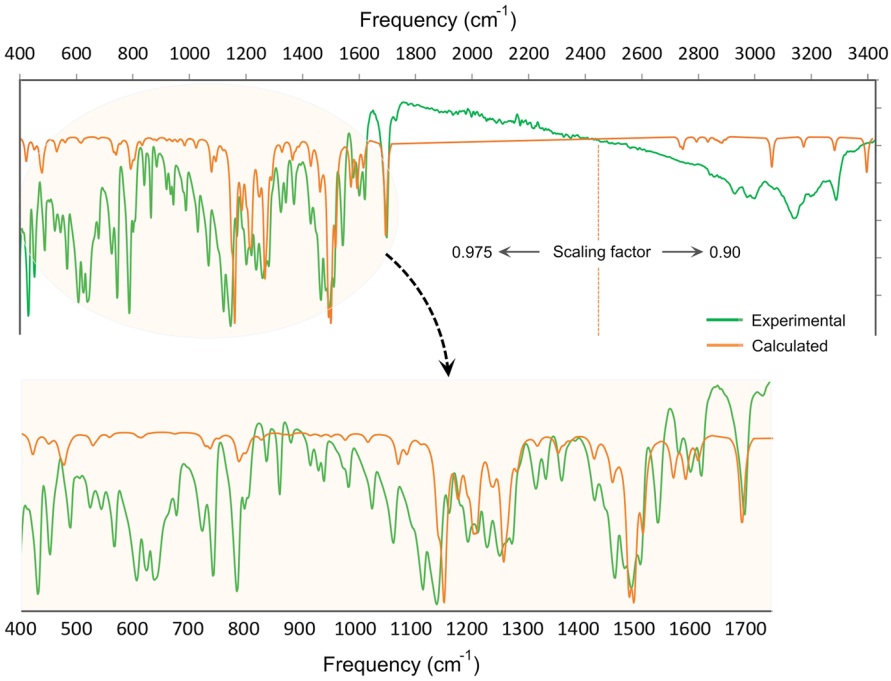

Fig. 1 Experimental and calculated IR peaks of compound **1**. Calculated IR values were scaled with a factor of 0.975 below the aromatic zone (for values < 3000 cm^{-1}) and with a factor of 0.90 for values above it

anharmonicity effects and therefore are given in Table 3 multiplied by scale factors of 0.91 for O–H, 0.90–0.91 for N–H, 0.96 for aromatic region, and 0.98 for C=O. In addition, since the deviation between the experimental and theoretical values in the low frequency region is very small, no scaling was carried out in this region.)

A comparison of experimental FTIR values of compound **1** with calculations is given in Fig. 1. The corresponding comparative figures for compounds **2–7** are provided in Supplementary Figure S22. To fix the experimental and theoretical results, the calculations were scaled with 0.975 below the aromatic region and 0.9 above it. The frequency data for all of the compounds were consistent with those reported for similar compounds in the literature [6, 22, 45, 46].

Interpretation of ^{1}H NMR spectra

The ^{1}H NMR spectra of all compounds were attained in DMSO-d_6 solution, and the chemical shifts, experimentally and theoretically, are summarized in Table 4, 5. In all spectra, the DMSO-d_6 were seen at around 2.00 and 2.55 ppm (quintet) and 3.40 ppm (variable, depending on the solvent and concentration), respectively [47]. For compounds **1–7**, the proton signals of the imine (–CH=N) were observed as singlets in the ranges 7.83–8.44 ppm. The –NH proton signals of the

Table 4 Experimental ^{1}H NMR values of the compounds (δ, ppm)

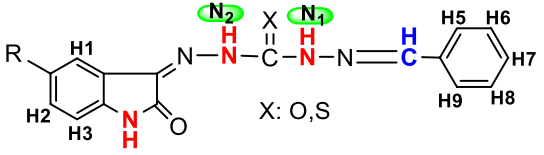

Comp	–CH=N	=N–N^{1}H	–N^{2}H–N	Isatin NH	Isatin H	ArH	–OH	–CH$_3$/OCH$_3$
1	8.06 (s, 1H)	12.48 (s, 1H)	> 14.00 (s, 1H)	11.26 (s, 1H)	7.57–7.55 (d, 1H, H1) 7.38–7.33 (t, 1H, R), 7.14–7.06 (dd, 2H, H2,H3)	7.67 (s, 1H, H5), 6.95–6.93 (d, 1H, H9) 6.83–6.80 (d, 1H, H8)	9.68 (s, 1H)	3.91 (s, 3H)
2	8.05 (s, 1H)	12.56 (s, 1H)	> 14.00(s, 1H)	11.25 (s, 1H)	7.57–7.55 (d, 1H, H1), 7.38–7.33 (t, 1H, R), 7.12–7.07 (t, 1H, H2), 6.95–6.93 (d, 1H, H3)	7.23 (s, 2H, H5,H9)	9.01 (s, 1H)	3.87 (s, 6H)
3	8.44 (s, 1H)	12.39 (s, 1H)	> 14.00 (s, 1H)	11.30 (s, 1H)	7.60–7.57 (d, 1H, H1), 7.41–7.36 (t, 1H, R), 7.14–7.09 (t, 1H, H2), 6.98–6.95 (d, 1H, H3)	7.94–7.91 (d, 1H, H8) 6.36–6.35 (d, 1H, H9) 6.32(s, 1H, H6)	10.03 (s, 1H), 9.96 (s, 1H)	–
4	8.07 (s, 1H)	12.50 (s, 1H)	> 14.00 (s, 1H)	11.23 (s, 1H)	7.60–7.58 (d, 1H, H1), 7.42–7.37 (t, 1H, R), 7.15–7.10 (t, 1H, H2), 7.00–6.98 (d, 1H, H3)	7.68 (s, 1H), 7.15–7.13 (d, 1H), 6.87–6.84 (d, 1H)	9.63 (s, 1H)	4.24–4.17 (q, 2H), 1.46–1.41 (t, 3H)
5	7.83 (s, 1H)	11.28 (s, 1H)	13.62 (s, 1H)	11.22 (s, 1H)	7.48 (s, H1), 7.36–7.33 (d, 2H, H2,H3)	7.23 (s, H5), 6.97– 6.92 (d, 2H, H8,H9)	9.07 (s, 1H)	3.80 (s, 3H)
6	7.86 (s, 1H)	11.37 (s, 1H)	13.74 (s, 1H)	11.33 (s, 1H)	7.50 –7.45 (d, 1H, H1), 7.40 – 7.36 (dd, 1H, H2), 6.96–6.93 (d, 1H, H3)	7.15 (s, 2H, H5,H9),	8.87 (s, 1H),	3.87 (s, 6H)
7	7.98 (s, 1H)	11.44(s, 1H)	13.71 (s, 1H)	11.33 (s, 1H)	7.81–7.78 (d, 1H, H2) 7.50 (s, 1H, H1) 6.96–6.93 (d, 1H, H3)	7.46–7.42 (3H, H6–H8), 7.38–7.35 (2H, H5,H9)	–	–

Table 5 Calculated ^{1}H NMR values of the compounds (δ, ppm)

Comp	–CH=N	=N–N^{1}H	–N^{2}H–N	Isatin NH	Isatin H	ArH	–OH	–CH_3/OCH_3
1	7.61	10.21	14.53	7.46	8.10 (H1) 7.52 (1H, R), 7.80, 7.33 (H2,H3)	7.69 (H5) 7.46 (H9) 7.44 (H8)	6.36	4.46–4.05
2	7.92	9.18	14.68	7.50	8.14 (H1) 7.47 (1H, R), 7.81, 7.33 (H2,H3)	7.19 (H5) 7.98 (H9)	6.19	4.50–3.64
3	8.13	9.08	14.27	7.51	8.17 (H1) 7.52 (1H, R), 7.78, 7.33 (H2,H3)	7.54 (H5) 6.73 (H6) 6.90 (H8)	9.74 (OH9) 5.24 (OH7)	–
4	7.65	10.20	14.52	7.49	8.10 (H1) 7.53 (1H, R), 7.79, 7.30 (H2,H3)	7.63 (H5) 7.43 (H8) 7.40 (H9)	6.43	4.43, 4.28 (2H), 1.66–1.51 (3H)
5	7.65	9.02	13.80	7.51	7.99 (H1) 7.66 (H2) 7.22 (H3)	7.54 (H5) 7.42 (H8) 7.36 (H9)	6.32	4.40–4.01
6	7.57	9.13	13.78	7.55	7.97 (H1) 7.64 (H2) 7.21 (H3)	7.46 (H5) 7.18 (H9)	6.27	4.42–3.60
7	7.77	9.22	13.82	7.48	8.04 (H1) 7.70 (H2) 7.19 (H3)	8.28 (H5) 7.96 (H6) 7.93 (H7) 8.03 (H8) 7.86 (H9)	–	–

isatin ring were detected as singlets in the ranges 11.22–11.33 ppm. The –N^1H and –N^2H proton signals of the thio/carbohydrazone moiety were detected as singlets in the ranges > 14.00–13.62 and 11.28–12.56 ppm, respectively. The aromatic proton (H1–H3) of the isatin ring was observed at 6.93–7.81 ppm. The aldehydic aromatic proton (H5–H9) was detected at between 6.32 and 7.94 ppm for all compounds. (All ^{1}H NMR spectra are given in Figs. S8–S14.) For compounds **1–6**, the –OH proton peaks were appeared as singlets in the ranges 8.87–10.03 ppm. For compounds **1**, **2**, **5** and **6**, the proton signals of the methoxy group (–OCH_3) appeared as a singlet at 3.91, 3.87, 3.80, and 3.87 ppm, respectively. For compound **4**, the proton signal of the methylene group (–OCH_2) was observed as a quartet at 4.17–4.24 ppm (2H, q); the –CH_3 proton signal was detected as a triplet at 1.41–1.46 ppm (3*H*, *t*). These results are consistent with values reported for similar compounds in the literature [5, 22, 45, 48].

Table 6 Experimental and calculated ^{13}C NMR values of the compounds (δ, ppm)

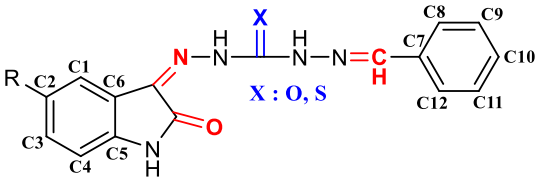

	Comp. **1**	Comp. **2**	Comp. **3**	Comp. **4**	Comp. **5**	Comp. **6**	Comp. **7**
Ist C=O	163.32	163.30	163.36	163.26	163.25	163.25	163.29
Ist C=N	145.30	142.79	142.69	145.34	143.73	148.80	141.66
C=X	175.37	175.39	174.94	175.37	151.84	151.81	151.20
–CH=N	142.77	139.02	142.40	142.79	141.63	140.93	140.94
C1	123.91	124.42	123.19	123.79	122.77	124.96	129.46
C2	123.21	123.21	121.35	123.20	127.19	127.17	130.66
C3	131.93	131.94	128.05	131.93	130.72	130.68	130.81
C4	120.81	120.81	120.84	120.83	120.40	120.36	113.16
C5	138.13	138.18	137.77	138.09	140.98	138.26	134.66
C6	115.98	111.76	112.12	116.01	113.96	113.07	113.37
C7	125.63	121.43	111.76	125.59	127.53	122.81	131.53
C8	109.52	105.74	161.95	110.41	112.47	105.00	127.46
C9	148.99	148.87	102.93	148.16	150.24	151.85	127.23
C10	150.25	145.25	159.48	150.41	147.34	158.42	120.43
C11	111.77	148.87	108.90	111.77	113.13	151.85	127.23
C12	121.41	105.74	131.85	121.41	120.17	105.00	127.46
CH_3/OCH_3/ CH_2	56.36	56.77	–	64.52, 15.43	56.32	56.66	–

Table 7 Calculated ^{13}C NMR values of the compounds (δ, ppm)

	Comp. **1**	Comp. **2**	Comp. **3**	Comp. **4**	Comp. **5**	Comp. **6**	Comp. **7**
Ist C=O	168.78	168.59	168.67	168.43	168.64	168.67	168.42
Ist C=N	143.48	144.14	143.63	143.04	139.61	139.66	139.70
C=X	185.92	184.09	182.30	185.84	158.92	158.87	158.47
–CH=N	149.48	151.78	155.74	150.03	148.19	147.90	147.57
C1	126.99	127.08	127.33	127.04	125.86	125.84	126.06
C2	128.51	128.41	128.70	128.45	141.96	141.94	142.13
C3	138.19	138.25	138.59	138.10	136.39	136.30	136.62
C4	115.85	115.46	115.73	115.96	116.94	116.88	116.85
C5	149.41	148.59	148.85	149.18	146.92	146.89	147.00
C6	127.16	127.45	126.99	127.13	129.39	129.51	129.43
C7	127.81	130.80	115.88	128.06	128.51	127.64	136.92
C8	112.64	127.28	142.48	112.66	112.64	107.80	131.61
C9	153.80	153.60	112.18	153.45	153.50	155.15	134.90
C10	157.25	151.64	169.39	156.65	156.19	150.31	136.70
C11	119.83	156.54	106.85	120.00	119.63	154.62	135.99
C12	131.24	106.43	169.10	131.66	130.37	125.84	137.03
CH_3/OCH_3/ CH_2	58.01	63.63, 58.89	–	69.14, 15.90	57.91	63.40, 58.12	–

Interpretation of ^{13}C NMR spectra

The ^{13}C NMR spectra of the compounds were taken in DMSO-d_6, and the chemical shifts, experimentally and theoretically, are summarized in Table 6, 7. For compounds **1–7**, the –C=N and –C=O carbon signals of the isatin ring were detected in the ranges 141.66–148.80 and 163.25–163.36 ppm, respectively. The –C=N of the imines unit were observed in the ranges 139.02–142.79 ppm. For compounds **1–7**, the –C=S and –C=O carbon signals (–C=X) of the thio/carbohydrazone moiety were detected in the ranges 174.94–175.39 and 151.20–151.84 ppm, respectively. For all compounds, the aromatic carbon atoms (C1–C6) of the isatin ring were observed at 111.76–140.98 ppm. The aldehydic aromatic proton (C7–C12) was detected at between 102.93 and 161.95 ppm (all ^1H NMR spectra are given in Figs. S15–S21).

The carbon atoms of the methoxy groups (–OCH_3) of compounds **1**, **2**, **5**, and **6** were resonated at 56.36, 56.77, 56.32, and 56.66 ppm, respectively. For compound **4**, the carbon atoms of the –OCH_2 and –CH_3 group were detected at 64.52 and 15.43 ppm. The some carbon signals were downfield shifted due to the presence of the hydroxide (–OH), methoxy (–OCH_3), and ethoxy (–OC_2H_5) group. These data are in agreement with ^{13}C NMR spectral results of similar compounds [5, 22, 45, 48].

Table 8 Results of DPPH, ABTS, and CUPRAC activity of the synthesized compounds

Comp	*R*	DPPH• (IC_{50}, μM)	ABTS•+ (IC_{50}, μM)	CUPRAC ($A_{0.50}$, μM)
1	3-OMe, 4-OH	37.20 ± 1.18	9.36 ± 0.33	9.68 ± 0.02
2	3,5-di-OMe, 4-OH	38.17 ± 0.44	9.68 ± 0.40	9.83 ± 0.01
3	2,4-di-OH	27.13 ± 0.35	6.47 ± 1.33	9.04 ± 0.02
4	3-OEt, 4-OH	38.00 ± 0.93	9.43 ± 1.42	9.64 ± 0.02
5	3-OMe, 4-OH	43.14 ± 0.87	24.96 ± 0.80	11.03 ± 0.04
6	3,5-di-OMe, 4-OH	43.35 ± 0.76	24.41 ± 0.51	10.16 ± 0.02
7	H	na	na	47.52 ± 0.05
BHA	–	9.55 ± 0.36	3.42 ± 0.04	2.24 ± 0.05

na not activated

Antioxidant activity

The results of DPPH, ABTS, and CUPRAC activity of the synthesized compounds are given in Table 8. The antioxidant activity results displayed six of seven compounds (except **7**, having no substituent) exhibited antioxidant properties for each assay. These compounds (**1–6**) showed DPPH and ABTS activities with the IC_{50} values ranging from 27.13 to 43.35 μM and 6.47 to 24.96 μM, respectively, whereas all compounds (**1**–**7**) exhibited CUPRAC activity with the $A_{0.50}$ values ranging from 9.04 to 47.52 μM. All antioxidant activities of them were lower than that of BHA (IC_{50} = 9.55 μM for DPPH, 3.42 μM for ABTS and $A_{0.50}$ = 2.24 μM for CUPRAC), used as a standard (Table 8).

The synthesized isatin-carbohydrazone derivatives, in this study, exhibited stronger DPPH activity than bis-carbohydrazones (IC_{50} values of them ranging from 51.82 μM to not active), whereas isatin-thiocarbohydrazones showed almost similar DPPH activity to bis-thiocarbohydrazones (IC_{50} values of them average approx. 30 μM), synthesized in our previous work [45]. The isatin-carbohydrazones, synthesized in this study, exhibited similar or lower ABTS activity than bis-carbohydrazones (IC_{50} values of them ranging from 7.4 to 164.16 μM) [45], while better ABTS activity than bis-isatin urea derivatives (IC_{50} values of them not active), synthesized in our previous work [6]. On the other hand, isatin-thiocarbohydrazones, in this study, showed stronger ABTS activity than bis-isatin thiourea derivatives (IC_{50} = 18.44–27.38 μM) [6], whereas weaker ABTS activity than bis-thiocarbohydrazones (IC_{50} = 2.69–5.32 μM) [45]. Furthermore, all synthesized isatin-(thio)/carbohydrazones have similar CUPRAC activity to bis-(thio)/carbohydrazones ($A_{0.50}$ = 3.18 μM–na) [45], while lower than bis-isatin urea/ thiourea derivatives ($A_{0.50}$ = 0.60–0.81 μM) [6].

From Table 8, the structure–activity relationship (SAR) can be observed as follows:

(i) Generally, all synthesized compounds (except **7** for ABTS assay) showed better CUPRAC and ABTS than DPPH activity. Additionally, thiocarbohydrazones (**1**–**4**) exhibited higher antioxidant activity than carbohydrazones (**5**–**7**) for

each assay. It is considered that this effect is due to the high polarizability and electron accepting ability of the S atom.

(ii) Among the synthesized compounds, as expected, compound **3**, having two hydroxyl groups as substituent, was found to be the best antioxidant agent for each assay (IC_{50} = 27.13 μM for DPPH, 6.47 μM for ABTS and $A_{0.50}$ = 9.04 μM for CUPRAC). On the other hand, compound **7**, containing no substituent on the phenyl ring, has only CUPRAC property ($A_{0.50}$ = 47.52 μM), while not active for DPPH and ABTS assays.

(iii) The binding of the second methoxy group to the phenyl ring did not have a remarkable effect on the antioxidant activities (compare compound **1** (*R* = 3-OMe, 4-OH; IC_{50} = 37.20 μM for DPPH, 9.36 μM for ABTS and $A_{0.50}$ = 9.68 μM for CUPRAC) with compound **2** (*R* = 3,5-di-OMe, 4-OH; IC_{50} = 38.17 μM for DPPH, 9.68 μM for ABTS and $A_{0.50}$ = 9.83 μM for CUPRAC), and compound **5** (*R* = 3-OMe, 4-OH; IC_{50} = 43.14 μM for DPPH, 24.96 μM for ABTS and $A_{0.50}$ = 11.03 μM for CUPRAC) with compound **6** (*R* = 3,5-di-OMe, 4-OH; IC_{50} = 43.35 μM for DPPH, 24.41 μM for ABTS and $A_{0.50}$ = 10.16 μM for CUPRAC)).

(iv) The attaching of the ethoxy group instead of methoxy to the phenyl ring did not significantly affect the antioxidant activity (compare compound **1** (*R* = 3-OMe, 4-OH; IC_{50} = 37.20 μM for DPPH, 9.36 μM for ABTS and $A_{0.50}$ = 9.68 μM for CUPRAC) with compound **4** (*R* = 3-OEt, 4-OH; IC_{50} = 38.00 μM for DPPH, 9.43 μM for ABTS and $A_{0.50}$ = 9.64 μM for CUPRAC)).

The presence of the phenolic moiety is important for the antioxidant agent, as phenols can be easily oxidized to quinones by accepting electron from radicals [6, 49, 50]. The SAR results support that the antioxidant properties of the synthesized compounds are realized by the electron capture of the hydroxyl group on the phenyl ring. This oxidation is important for antioxidant agents, because quinones, having antitumor properties, can hinder to occur oxygen radicals that cause DNA damage. The predicted oxidation mechanism of compound **3**, which is the best antioxidant agent in this study, is given in Scheme 2.

It is well known that the hydroxyl group as a substituent is important for the antioxidant agent because of its oxidation ability. On the other hand, while the isatin-thiocarbohydrazones, synthesized in this study, are compared with bis-thiocarbohydrazones and bis-isatin thiourea, synthesized our previous work [6, 45], bis-thiocarbohydrazones have the strongest DPPH and ABTS activities. It is considered that the increased phenolic groups may rise the antioxidant properties due to enhancing electron carrying capacity.

Theoretical analysis

Among the reaction types that occur between antioxidant compounds and free radicals, hydrogen atom transfer (HAT) and single electron transfer (SET) mechanisms, both of which can occur simultaneously, appear as primary reaction mechanism types. In the reaction mechanism of HAT given as DPPH• + RH → DPPH + R, the antioxidant activity of a compound is determined by the oxidation of DPPH• in the test sample. The higher antioxidant activity of the compound is proportional to the

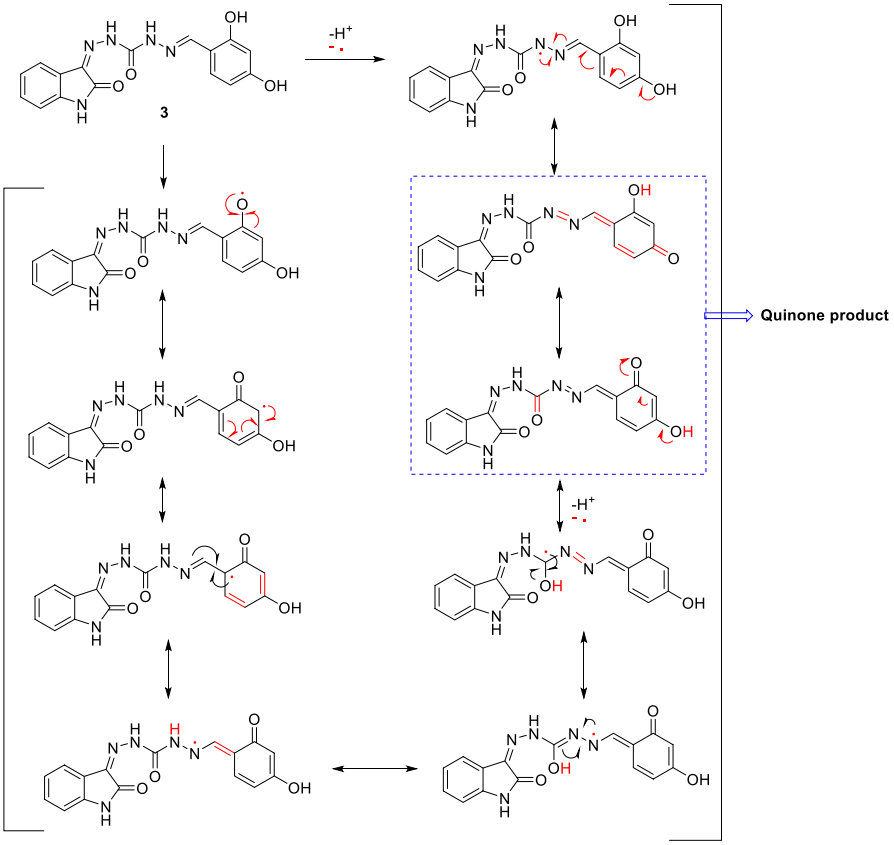

Scheme 2 Predicted oxidation mechanism of compound **3** to quinone

presence of its weak hydrogen bonds. The effectiveness of the HAT mechanism is evaluated by the ability of the free radical to remove a hydrogen atom of the antioxidant, so that, in addition to the electronic properties of the reactants such as NH, OH, bond dissociation enthalpy, bond strength, electron density on the bond, the magnitude of the collision probability of the compound with DPPH• in appropriate coordination (i.e., the volumetric sizes of the substituents and bonded groups to minimize the steric effect) and their conformational orientations also have an important role in the evaluation of the antioxidant effect. In this context, since the probability of the occurrence of HAT depends on the instantaneous appropriate values of many parameters, the most probable estimates of the HAT mechanism of the antioxidant characteristic of a compound have difficulties due to limitations in both experimental observations and calculations.

SET is a mechanism that describes electron transfer from nucleophile to substrate, and can be defined by $\mathrm{DPPH}\cdot + R \rightarrow \mathrm{DPPH}^{-} + R^{+}\cdot$ In most cases, HAT and SET reactions occur simultaneously in a reaction and it is difficult to distinguish these mechanisms. Ionization energy is the amount of energy required to remove an

electron from a molecule's HOMO, and low ionization potential (IP) values of an antioxidant result in easier electron abstraction and, accordingly, higher antioxidant activity, and therefore, the IP of the antioxidant is an important parameter in determining antioxidant activity in SET reactions. Negative values of HOMO energy give information about the ionization potential and are expressed as IP = $-E_{\mathrm{HOMO}}$. Calculations revealed that the ionization potentials of the sulfur-centered compounds **1**–**4** are lower than that of the oxygen-centered compounds **5**–**7** (Supplementary Table S2). Moreover, electronegativity is defined as the tendency of an atom (or functional group) to attract electrons toward itself, and the electronegativity values of compounds **1**–**4** are smaller (except comp. **3**) than those of compounds **5**–**7** (Fig. 3b), indicating that they are more favored as electron donors. Although these reactivity parameters are not conclusive in determining the pathway of an antioxidant reaction mechanism, they can be helpful in understanding the type of reaction. In a rough approximation, the energy gap (ΔE) between HOMO and LUMO energies is directly proportional to the reactivity of a compound, that is, small ΔE means that the chemical hardness of the compound is low and its reactivity is high (see Fig. 2 for comp. **1** and **5**; see Supplementary Figure S23 for all of the compounds). In this regard, compounds **1**–**4** are expected to be more reactive than the others (see Fig. 3a).

The nucleophilicity indices of compounds **5**–**7** obtained using the $N_{(\mathrm{Nu})} = E_{\mathrm{HOMO(Nu)}} - E_{\mathrm{HOMO(TCE)}}$ approach [51] were found to be lower than those of compounds **1**–**4** (where TCE is tetracyanoethylene and its HOMO energy was calculated as −9.495 eV), indicating that compounds **1**–**4** are stronger electron donors

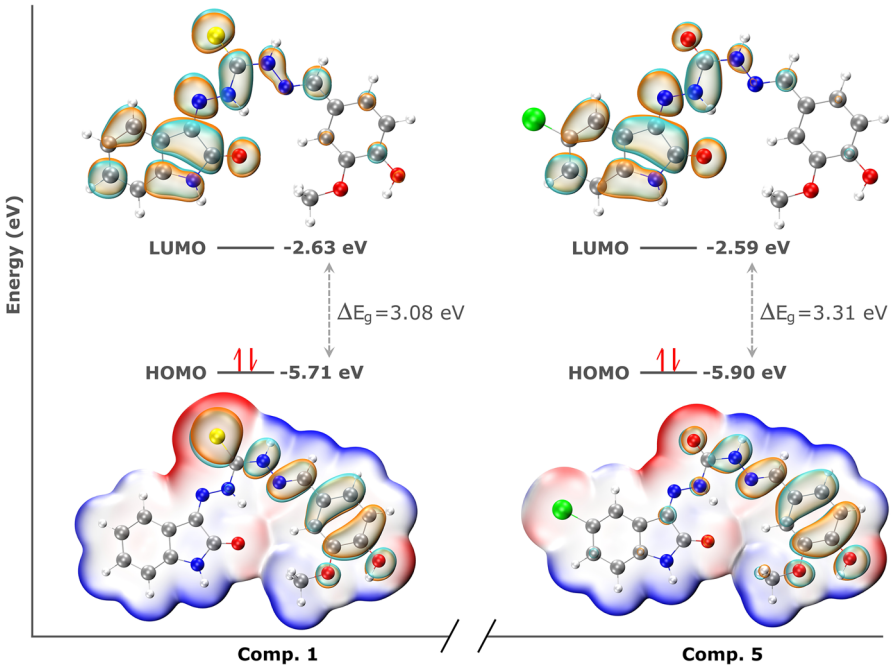

Fig. 2 HOMO-ESP and LUMO maps for compounds **1** and **5**

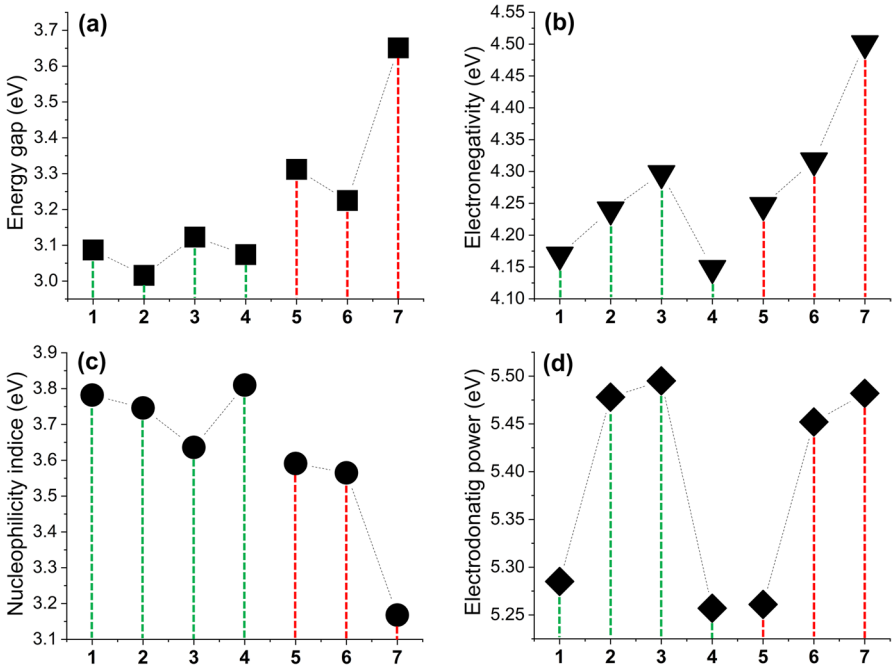

Fig. 3 Energy gap (ΔE), electronegativity (χ), nucleophilic index (ε), and electrodonating power (ω^-) data of the compounds

(Fig. 3c). Electrodonating power parameters ($\omega^- = I^2/2(I - A)$) [52] were calculated to support the reactions of the compounds via the SET mechanism (I: ionisation potential ($-E_{\mathrm{HOMO}}$), A: electron affinity ($-E_{\mathrm{LUMO}}$)). Calculations revealed that compounds **2**, **3** and **6**, **7** have higher electron donating capacity than other compounds (Fig. 3d). *o*- and *p*–OH-substituted compound **3** stands out as the compound with the highest both nucleophilic and electrodonating power parameters. Although the ω^- is considered as a measure of a compound's ability to donate electrons more easily, the displacement of an electron from HOMO to LUMO is directly related to ΔE. In this context, it can be said that sulfur-centered compounds can donate electrons more easily than oxygen-centered compounds, and thus, they can perform SET reactions more easily.

Single electron transfer enthalpy (SETE) calculations were carried out to examine the tendency of the compounds to SET reactions. With SETE calculations, the change in enthalpy of compounds when they lose an electron, that is, the energies required for them to donate an electron, was calculated. Antioxidant test results and SETE data for compounds **1**–**6** are given in Fig. 4. Experimental results revealed that compounds **1**–**4** showed higher antioxidant properties than other compounds. SETE calculations also showed that in parallel with the experimental data, compounds **1**–**4** would require lower energies for SET reactions. Both the experimental results ($A_{0.50}$=47.52 µM for CUPRAC) and SETE calculations (173 kcal/mol) of compound **7** reveal its low antioxidant property. The SETE calculation value for compound **3** has a noticeable deviation, which can be expected to be the lowest

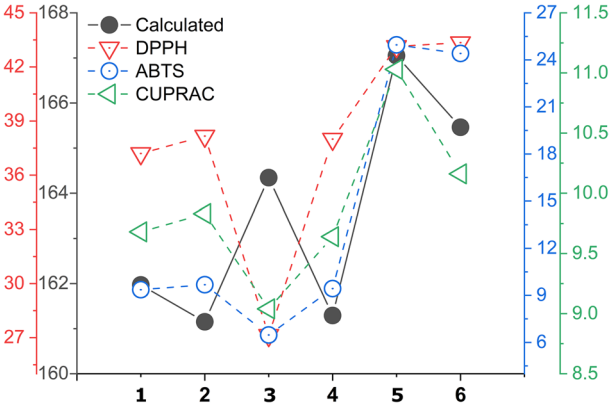

Fig. 4 Calculated single electron transfer enthalpy, SETE (kcal/mol), data, and experimental antioxidant results

value since it exhibits the highest antioxidant property, but the ΔE, χ, $N_{(Nu)}$ parameters obtained from FMO eigenvalues and SETE values showed similar behavior. In other words, in terms of the SET reaction, compound **3** has calculation results that are not considered the most active among compounds **1**–**4**. At this point, considering that the SET and HAT reactions occur together, it can be concluded that compound **3** shows a dominant HAT reaction. The presence of *o*-, *p*-hydroxyl groups on compound **3** supports this assumption. It is possible that the reactivity of the *p*-hydroxyl groups in other compounds occurred at a lower level due to the possible steric effect of the adjacent methoxy and ethoxy structures.

QTAIM calculations provide insight into the interatomic interactions in a chemical system. IRI analysis, on the other hand, is an effective tool for examining chemical bonds and weak interaction regions. Thus, IRI and QTAIM calculations were

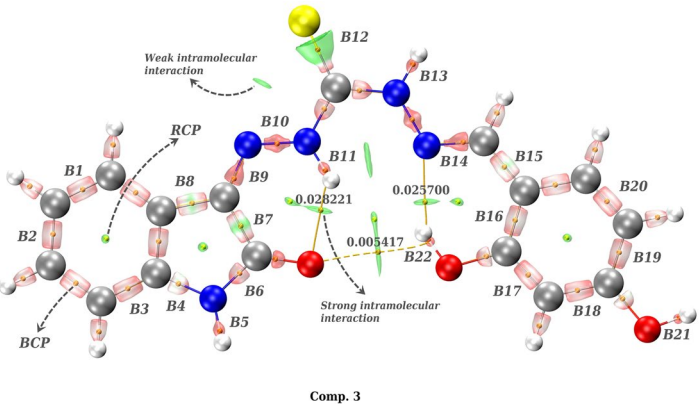

	Rho	DI
B1	0.311168	1.384142
B2	0.311084	1.384777
B3	0.317513	1.355403
B4	0.288941	1.013040
B5	0.347868	0.799240
B6	0.317881	1.045852
B7	0.261893	0.923826
B8	0.277813	1.062951
B9	0.371672	1.454975
B10	0.370330	1.353376
B11	0.340498	0.660613
B12	0.215193	1.590522
B13	0.346404	0.764693
B14	0.371104	1.463115
B15	0.283876	1.126831
B16	0.299695	1.211181
B17	0.316709	1.309599
B18	0.318719	1.319771
B19	0.309936	1.270289
B20	0.318675	1.431100
B21	0.374629	0.658373
B22	0.360091	0.532961

Fig. 5 IRI and QTAIM data for compound **3** (The unit of electron densities, Rho, calculated in BCP and RCP is e/bohr^3). Regions with higher electron density are red, and regions with less electron density are green, such as *B2* and *B7*

performed to analyze the bond properties of the compounds in more detail and to examine the effects of intramolecular interactions on the compounds. IRI function is defined as follows [53];

$$\mathrm{IRI}(r) = \frac{|\nabla \rho(r)|}{[\rho(r)]^{\alpha}}$$

where α is an adjustable parameter ρ and $\boldsymbol{r}$ represent electron density and coordinate vector, respectively. The IRI map of Compound **3** (Fig. 5; see Supplementary Figure S24 for all of the compounds) reveals strong intermolecular interactions for –C=O···HN (0.028221 e/bohr^3) and –N···HO– (0.025700 e/bohr^3), while weaker interactions for –C=O···HO– (0.005417 e/bohr^3).

IRI calculations provide great convenience especially for visual analysis of charge concentrations on carbon–carbon bonds. For example, it can be clearly seen in the IRI maps that the electron densities of *B7* and *B8* bonds (0.261893 *e*/bohr^3 and 0.277813 *e*/bohr^3) on the isatin are lower than those of *B1*, *B2* and *B3* (0.311168 *e*/bohr^3, 0.311084 *e*/bohr^3, and 0.317513 *e*/bohr^3, respectively), and this visual information is also supported by QTAIM data. In this respect, it can be seen directly on the IRI surfaces that the charge density on *B7* is higher than on B8. For carbon–nitrogen bonds, for example –N=C– (*B9* or *B14*) and –C–N– (*B4* or *B6*), there are noticeable differences among themselves. B9 with π-bond has the highest charge density (0.371672 *e*/bohr^3), followed by *B6* (0.317881 *e*/bohr^3) and *B4* (0.288941 *e*/bohr^3) bonds, respectively.

The charge densities on N–H (*B5*, *B11* or *B13*) and O–H (*B21* or *B22*) have the order $\rho_{B21} > \rho_{B22} > \rho_{B5} > \rho_{B13} > \rho_{B11}$, and the IRI surfaces support the idea that the charge density on B11 is weakened by –C=O···HN and –C=N–N···HN interactions. In addition, electron delocalization between atoms can be related to the electron density on the BCP. The delocalization index relates to the number of electron pairs shared by two atoms [54] and is therefore a parameter that somewhat reflects the covalentness of the bond, i.e., it has lower values in polar bonds. In this context, O–H is more polar than N–H and has a lower DI. The charge density on *B22* decreased due to the OH···N= and OH···O=C interactions, thus making the bond more polar. Accordingly, the DI value of *B22* was calculated to be smaller compared to *B21*. Although it is assumed that this may cause *B22* to behave more reactively in HAT reactions, the orientation of the *B22*(H) atom for the reaction can be restricted by intramolecular effects and it should not be ignored that it is highly likely to be exposed to steric effects due to its location.

Conclusion

New Schiff bases based on isatin and (thio)/carbohydrazone derivatives have been synthesized and isolated with good yields of 60–90% yields. The chemical structures of the compounds have been elucidated by FTIR, ^{1}H, and ^{13}C NMR spectroscopic approaches, and elemental analysis.

All synthesized compounds (**1–7**) exhibited CUPRAC activity with the $A_{0.50}$ values ranging from 9.04 to 47.52 μM, while compounds **1–6** exhibited DPPH and ABTS activities with the IC_{50} values ranging from 27.13 to 43.35 μM and

6.47 to 24.96 μM, respectively. Compound **3**, having two hydroxyl groups, showed the strongest antioxidant activity for each assay. Sulfur-centered structures (**1**–**4**) were found to have higher antioxidant activity than oxygen-centered structures (**5**–**7**) for each assay (DPPH, ABTS and CUPRAC).

HAT and SET reactions usually occur at the same time, and each mechanism is controlled by its own variables. While parameters such as bond strength, conformational orientation, and the probability of collision with DPPH• of reactive bonds are effective in HAT reactions, electronic parameters such as ionization potential, electronegativity, energy gap between HOMO and LUMO energies, nucleophilicity, electrodonating power, and single electron transfer enthalpy are important for SET reactions. The calculations revealed that the ionization potentials, electronegativity, and energy gap between HOMO and LUMO energies in general of the sulfur-centered compounds were lower than that of the oxygen-centered compounds and showed that the sulfur-centered compounds were more preferred as electron donors. In addition, compounds with larger nucleophilicity indices exhibited higher antioxidant behavior as strong electron donors. Electrodonating power parameters were also used to estimate the probabilities of the compounds to perform the SET reaction, and results were partially consistent with the experiment. In addition, the analysis of the electron donating ability of a compound over different parameters revealed that sulfur-centered compounds can donate electrons more easily than oxygen-centered compounds, and thus, they can perform SET reactions more easily. Consistent with the experimental results, single electron transfer enthalpy calculations also showed that sulfur-centered compounds would require lower energies than oxygen-centered compounds for SET reactions.

The compounds are structurally not very suitable for HAT reactions, but the presence of *o*-, *p*-hydroxyl groups, especially on compound **3**, strengthened the assumption that it showed a more dominant HAT reaction than other compounds. It is a strong assumption that the steric effect of methoxy and ethoxy structures reduced the reactivity of *p*-hydroxyl groups, and therefore, findings supporting SET reactions gained weight in the calculations. It has also emerged that a combination of QTAIM and IRI analyses can be an effective tool to analyze the bond properties of compounds in more detail and to examine both interatomic and intermolecular interaction sites.

Supplementary Information The online version contains supplementary material available at https://doi.org/10.1007/s11164-022-04908-1.

Acknowledgements The numerical calculations reported in this paper were partially performed at TUBITAK ULAKBIM, High Performance and Grid Computing Center (TRUBA resources).

Authors contribution HM involved in synthesis, spectroscopic characterization, writing, FS took part in biological studies, writing—review, MSÇ involved in theoretical calculations, writing—review, BZK involved in biological studies, writing—review, and HY involved in structure elucidation, writing—review, visualization, and editing. All authors reviewed the manuscript.

Funding This study was not supported by any organization.

Declarations

Conflict of interest The authors declare that they have no conflict of interest.

Ethics approval All of the material is owned by the authors and/or no permissions are required.

Consent for publication The results/data/figures in this manuscript have not been published elsewhere, nor are they under consideration by another publisher.

References

1. S. Alyar, T. Şen, Ü.Ö. Özmen, H. Alyar, Ş Adem, C. Şen, J. Mol. Struct. **1185**, 416 (2019)
2. S. Shukla, R. Srivastava, S. Shrivastava, A. Sodhi, P. Kumar, Med. Chem. Res. **22**, 1604 (2013)
3. S.S. Ali, E.-R. Kenawy, F.I. Sonbol, J. Sun, M. Al-Etewy, A. Ali, L. Huizi, N.A. El-Zawawy, Pharm. Res. **36**, 5 (2019)
4. L. Pogány, J. Moncol, J. Pavlik, M. Mazúr, I. Šalitroš, ChemPlusChem **84**, 358 (2019)
5. H. Muğlu, H. Yakan, A.G.A. Misbah, M.S. Çavuş, T.K. Bakır, Res. Chem. Intermed. **47**, 4985 (2021)
6. H. Yakan, M.S. Çavuş, B.Z. Kurt, H. Muğlu, F. Sönmez, E. Güzel, J. Mol. Struct. **1239**, 130495 (2021)
7. M.J. Kareem, A.A.S. Al-Hamdani, Y.G. Ko, W. Al Zoubi, S.G. Mohammed, J. Mol. Struct. **1231**, 129669 (2021)
8. A. Cinarli, D. Gürbüz, A. Tavman, A.S. Birteksöz, Bull. Chem. Soc. Ethiop. **25**, 407 (2011)
9. S. Pandeya, D. Sriram, G. Nath, E. De Clercq, Pharm. Acta Helv. **74**, 11 (1999)
10. A.S. Hassan, T.S. Hafez, S.A.M. Osman, M.M. Ali, Turk. J. Chem. **39**, 1102 (2015)
11. M.M. Abdelaal, S. Mohamed, Y. Barakat, H.A. Derbala, H.H. Hassan, W. Al Zoubi, Egypt. J. Chem. **61**, 539 (2018)
12. W. Al Zoubi, S.G. Mohamed, A.A.S. Al-Hamdani, A.P. Mahendradhany, Y.G. Ko, RSC Adv **8**, 23294 (2018)
13. K. Gangarapu, S. Manda, A. Jallapally, S. Thota, S.S. Karki, J. Balzarini, E. De Clercq, H. Tokuda, Med. Chem. Res. **23**, 1046 (2014)
14. M.T. Gabr, N.S. El-Gohary, E.R. El-Bendary, M.M. El-Kerdawy, N. Ni, Eur. J. Med. Chem. **128**, 36 (2017)
15. T. Aboul-Fadl, F.A. Bin-Jubair, O. Aboul-Wafa, Eur. J. Med. Chem. **45**, 4578 (2010)
16. M.T. Muhammad, N. Ghouri, K.M. Khan, M.I. Choudhary, S. Perveen, Med. Chem. **14**, 725 (2018)
17. G. Kiran, M. Sarangapani, T. Gouthami, A.R. Narsimha Reddy, Toxicol. Environ. Chem. **95**, 367 (2013)
18. K. Kumar, M. Kamboj, K. Jain, D. Singh, Spectrochim. Acta Part A Mol. Biomol. Spectrosc. **128**, 243 (2014)
19. H. Muğlu, H. Yakan, T.K. Bakir, Turk. J. Chem. **44**, 237 (2020)
20. T.K. Bakır, J.B. Lawag, Res. Chem. Intermed. **46**, 2541 (2020)
21. H. Muğlu, M.S. Çavuş, T. Bakır, H. Yakan, J. Mol. Struct. **1196**, 819 (2019)
22. H. Yakan, T.K. Bakır, M.S. Çavuş, H. Muğlu, Res. Chem. Intermed. **46**, 5417 (2020)
23. J.M. Mccord, Clin. Biochem. **26**, 351 (1993)
24. Y. Dai, C. Shao, Y. Piao, H. Hu, K. Lu, T. Zhang, X. Zhang, S. Jia, M. Wang, S. Man, Carbohydr. Polym. **178**, 34 (2017)
25. L. Overley, Free Radical Biol. Med. **5**, 113 (1988)
26. Y. Fang, Y. Sheng, W. Guoyao, Nutrition **18**, 872 (2002)
27. J. Moskovitz, M.B. Yim, P.B. Chock, Arch. Biochem. Biophys. **397**, 354 (2002)
28. S.J.K. Jensen, J. Mol. Struct. (Thoechem) **666**, 387 (2003)
29. J.D. Hayes, A.T. Dinkova-Kostova, K.D. Tew, Cancer Cell **38**, 167 (2020)
30. A. Pisoschi, I.F. Papa, P.G. StanceL, A. Serban, Eur. J. Med. Chem. **209**, 112891 (2021)
31. H. Sies, D.P. Jones, Nat. Rev. Mol. Cell Biol. **21**, 363 (2020)
32. N. Zhang, P. Hu, Y. Wang, Q. Tang, Q. Zheng, Z. Wang, Y. He, ACS Sensors **5**, 319 (2020)
33. M.V. Irazabal, V.E. Torres, Cells **9**, 1342 (2020)

34. A. Kirtonia, G. Sethi, M. Garg, Cell. Mol. Life Sci. **77**, 4459 (2020)
35. B.Z. Kurt, I. Gazioglu, N.O. Kandas, F. Sonmez, ChemistrySelect **3**, 3978 (2018)
36. B.Z. Kurt, I. Gazioglu, F. Sonmez, M. Kucukislamoglu, Bioorg. Chem. **59**, 80 (2015)
37. R. Apak, K. Güçlü, M. Özyürek, S.E. Karademir, J. Agric. Food Chem. **52**, 7970 (2004)
38. H. Yakan, S. Cakmak, H. Kutuk, S. Yenigun, T. Ozen, Res. Chem. Intermed. **46**, 2767 (2020)
39. P. Hohenberg, W. Kohn, Phys. Rev. **136**, B864 (1964)
40. W. Kohn, L.J. Sham, Phys. Rev. **140**, A1133 (1965)
41. M.J. Frisch, G. Trucks, H. Schlegel, G. Scuseria, M. Robb, J. Cheeseman, G. Scalmani, V. Barone, B. Mennucci, G. Petersson, Inc. Wallingford, CT, (2009)
42. T. Lu, F. Chen, J. Comput. Chem. **33**, 580 (2012)
43. R.F. Bader, Acc. Chem. Res. **18**, 9 (1985)
44. R.F. Bader, Chem. Rev. **91**, 893 (1991)
45. H. Muğlu, B.Z. Kurt, F. Sönmez, E. Güzel, M.S. Çavuş, H. Yakan, J. Phys. Chem. Sol. **164**, 110618 (2022)
46. M.S. Çavuş, H. Yakan, H. Muğlu, T. Bakır, J. Phys. Chem. Solids **140**, 109362 (2020)
47. I. Fleming, D. Williams, *Spectroscopic methods in organic chemistry*, 7th edn. (Springer Nature, Switzerland, 2020)
48. H. Muğlu, M. Akın, M.S. Çavuş, H. Yakan, N. Şaki, E. Güzel, Comput. Biol. Chem. **96**, 107618 (2022)
49. G. Powis, Free Radical Biol. Med. **6**, 63 (1989)
50. F. Sonmez, Z. Gunesli, B.Z. Kurt, I. Gazioglu, D. Avci, M. Kucukislamoglu, Mol. Divers. **23**, 829 (2019)
51. L.R. Domingo, E. Chamorro, P. Pérez, J. Org. Chem. **73**, 4615 (2008)
52. L.R. Domingo, P. Pérez, Org. Biomol. Chem. **9**, 7168 (2011)
53. T. Lu, Q. Chen, Chemistry-Methods **1**, 231 (2021)
54. X. Fradera, M.A. Austen, R.F. Bader, J. Phys. Chem. A **103**, 304 (1999)

Authors and Affiliations

Halit Muğlu[1] · Fatih Sönmez[2] · M. Serdar Çavuş[3] · Belma Z. Kurt[4] · Hasan Yakan[5]

✉ M. Serdar Çavuş
mserdarcavus@kastamonu.edu.tr

✉ Hasan Yakan
hasany@omu.edu.tr

1 Department of Chemistry, Kastamonu University, Kastamonu, Turkey

2 Pamukova Vocational School, Sakarya University of Applied Sciences, Sakarya, Turkey

3 Biomedical Engineering Department, Faculty of Engineering and Architecture, Kastamonu University, Kastamonu, Turkey

4 Department of Pharmaceutical Chemistry, Faculty of Pharmacy, Bezmialem Vakif University, Istanbul, Turkey

5 Chemistry Education, Faculty of Education, Ondokuz Mayıs University, Samsun, Turkey